Springwater pallasite (a stony-iron meteorite) showcasing gem-quality olivine in iron-nickel metal with hints of the Widmanstätten exsolution pattern.

1811-5209/23/0019-0173\$2.50 DOI: 10.2138/gselements.19.3.173

livine occurs across the galaxy, from Earth to extraterrestrial bodies including the Moon, Mars, and asteroids, to particles of comet dust and distant debris disks. The mineral is critical to our understanding of early Solar System chronology, planetary formation processes (e.g., magma ocean solidification), crustal evolution (e.g., volcanic eruptions), and surface weathering. Olivine's ability to shed light on these processes lies in the linkage of small, physical samples and satellite-derived data. Laboratory spectra become the basis for olivine detection and compositional interpretation in remotely sensed spectra ranging from high-resolution planetary maps to single extrasolar datapoints. In turn, petrologic studies of olivine underpin the geologic interpretations of these spectral datasets. Finally, olivine chemistry records Solar System formation conditions and relative chronology. Olivine is our bridge across time and space.

KEYWORDS: olivine; early Solar System; Moon; Mars; Venus; exoplanets; presolar grains; remote sensing; spectroscopy; planetary evolution

INTRODUCTION

One of the most distant detections of olivine ever made is also one of the most primordial. Far infrared spectra reveal the presence of olivine in a debris disk around the bright, young star Beta Pictoris, with a composition similar to that of olivine from comets in our own Solar System (de Vries et al. 2012). This distant disk, 600 trillion km from home, bears witness to the universality of olivine as an early and essential building block of terrestrial planets (Fig. 1). Olivine has been identified in every known type of extraterrestrial material, from planets to moons, asteroids, comets, and interstellar dust grains. Its shape records thermal history; its composition is sensitive to thermodynamic variables (T, P, fO₂) and radiometric age; its abundance on planetary surfaces reflects interior dynamics and volcanism; even as it weathers away, olivine broadcasts timescales of surface alteration.

In this article, we explore planetary processes as recorded by olivine, via remotely sensed data, in situ measurements, and numerical modeling. We leave Earth's olivine to the rest of this issue, focusing instead on major Solar System bodies and recent exoplanet work, leaving outer Solar System objects, other moons, and a large body of astronomical studies for another review. Visible to near-infrared (VNIR) and thermal infrared (TIR) spectroscopy methods are used for every material we discuss, so we dedicate Box 1 to explaining them. Though not mentioned explicitly here, most elemental compositions of olivine samples in meteorites or returned materials

are determined via electron microprobe analysis. Below, we trace key findings and exciting new work on the fundamental planetary processes revealed by the study of olivine, arranged broadly from bodies that record the earliest Solar System formation events to those that are geologically active today, to those outside the Solar System.

OLIVINE IN EARLY SOLAR SYSTEM MATERIALS

Presolar Grains

Our Solar System was born ~4.6 Ga, from a region of gas and dust left behind by older, dying stars (Fig. 1 TOP LEFT). The collapse of this molecular cloud created the proto-Sun, followed immediately by the coalescence of tiny dust grains to form rocky particles and eventually planetesimals—the building blocks of planets. Although each precursor star had a unique isotopic composition, mixing in the nebula homogenized these isotopic fingerprints into a single "solar" composition, leaving few clues as to the presolar origins of our Sun and planets. But scientists discovered tiny (nanometer to micrometer scale) particles of ancient stardust buried in meteorites, comets, and even floating in space (e.g., Nittler and Ciesla 2016). These presolar grains contain a variety of materials, from nanocrystals of diamond to spinel, and even olivine (Fig. 1 TOP LEFT INSET). The oxygen isotope ratios ($^{18}O/^{16}O$ and $^{17}O/^{16}O$) of these olivine grains, determined via nano secondary ion mass spectrometry (NanoSIMS), differ greatly from solar and point to formation in specific stellar environments, including older, massive stars and supernovae. These O isotope ratios, combined with other isotopic systematics and basic Fe-Mg composition, can even pinpoint the size

¹ Macalester College Geology Department Saint Paul, MN 55105, USA E-mail: efirst@macalester.edu

² Stony Brook University Department of Geosciences Stony Brook, NY 11794, USA E-mail: christopher.h.kremer@stonybrook.edu

³ University of California Santa Cruz
Earth and Planetary Sciences Department
Santa Cruz, CA 95064, USA
E-mail: mtelus@ucsc.edu

⁴ University of Hawai'i at Mānoa Hawai'i Institute of Geophysics and Planetology Honolulu, HI 96822, USA E-mail: dtrang@higp.hawaii.edu

of a supernova and indicate within which nucleosynthetic mixing zones the olivine grain formed (Messenger et al. 2005).

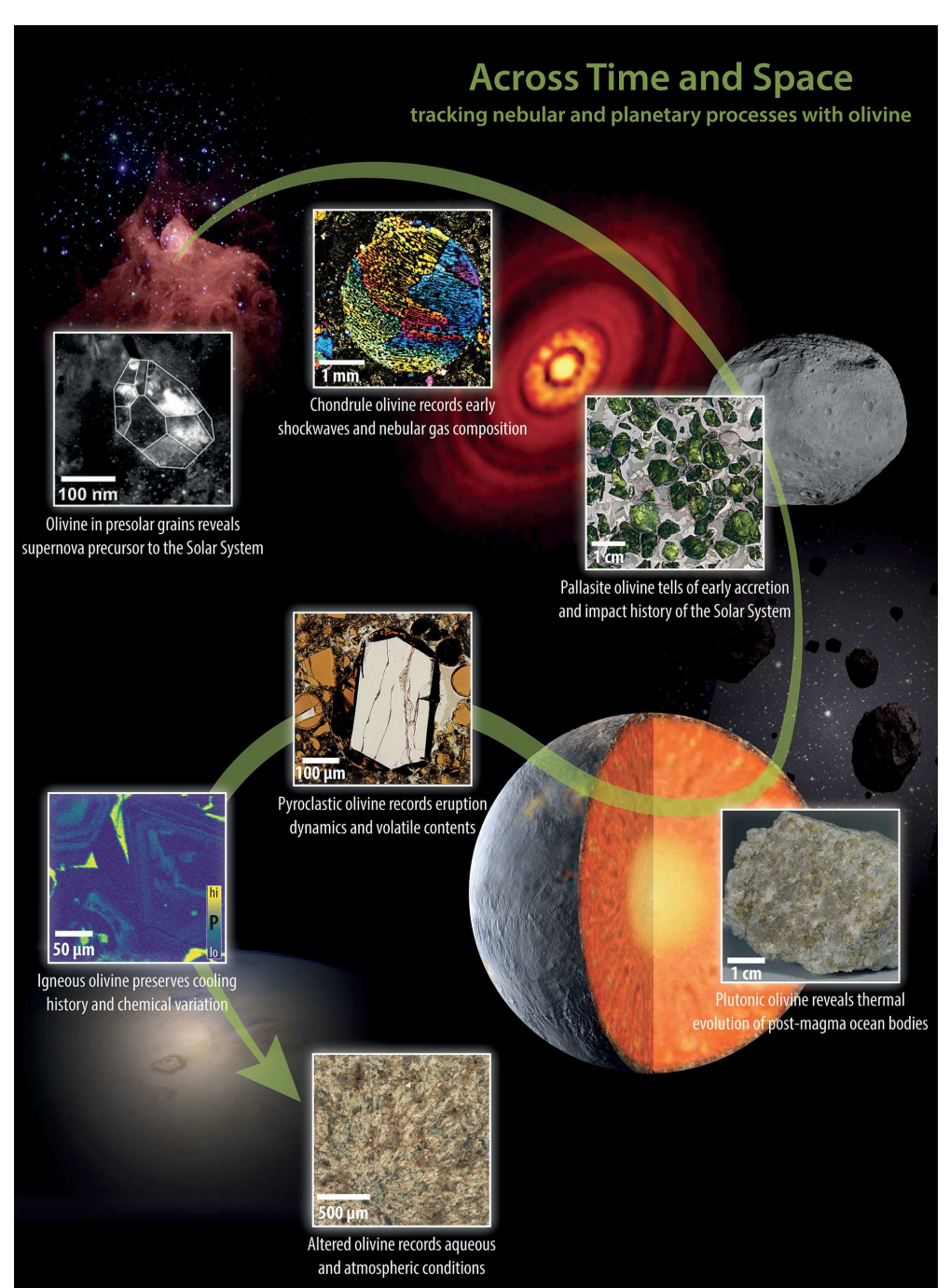
Chondrules and Chondrites

As the Solar System developed in earnest, dust came together to form larger particles, which merged again and again in the process of planetary accretion (the protoplanetary disk period). It was during this time, 1–3 My after the birth of the Sun, that millimeter-sized spheres of primi-

tive minerals and melt, or chondrules, formed (FIG. 1 TOP MIDDLE INSET). These chondrules, composed largely of crystalline olivine and pyroxene, are the main constituents of chondrite meteorites. Canonically, chondrules are interpreted to have formed when transient heating events caused dusty aggregates to melt at temperatures of 1400–1800 °C, forming droplets that cooled at rates from 10 to 1000 °C/h, resulting in a variety of igneous textures (e.g., Nittler and Ciesla 2016). Matching the morphology of chondrule olivine to the morphology of olivine grown

at different cooling rates, experiments show that most chondrule textures can be produced over a wide range of cooling rates, except the rapidly cooled barred olivine (BO) chondrules. However, a new experimental study reproduces the textural hallmarks of BO chondrules, including parallel bars of olivine and ovoid melt inclusions, at cooling rates of ≤10 °C/h (Faure et al. 2022). This work brings the BO chondrules into alignment with other textural types, suggesting that all chondrules could have cooled over days rather than minutes to hours. Other recent work highlights subtle chemical patterns in chondrule olivine, observed by cathodoluminescence, that suggest their crystallization is controlled by liquid interaction with Mg- and Si-rich gas, with the tantalizing implication that nebular gas compositions are thus recorded by chondrule olivine (Libourel and Portail 2018).

Most chondrules eventually became incorporated into kilometer-sized objects called planetesimals, where heat from the decay of ²⁶Al (a now extinct radionuclide with $t_{1/2} = 717,000$ y) caused varying degrees of thermal metamorphism, tracked by olivine composition and abundance (e.g., Vernazza et al. 2015). Planetesimals that formed beyond Jupiter are thought to be the parent bodies of carbonaceous chondrite meteorites (e.g., CM, CR, and CI types; Nittler and Ciesla 2016). These carbonbearing planetesimals accreted significant amounts of ice that eventually resulted in fluid alteration marked by conversion of chondrule olivine to serpentine.



Olivine records nebular and planetary processes across the galaxy. Following the arrow, inset images are: presolar olivine grain, TEM (MESSENGER ET AL. 2005); Maralinga barred olivine (BO) chondrule, crossed polars (PHOTO: LAURENCE GARVIE, BUSECK CENTER FOR METEORITE STUDIES, ASU); Seymchan pallasite (PHOTO: LAURENCE GARVIE); lunar troctolite 76535 (NASA); Apollo 17 orange glass deposit, transmitted light (PHOTO: EMILY FIRST); phosphorous distribution in olivine in Martian meteorite Yamato 980459 (PHOTO: EMILY FIRST); Dourbes abrasion patch on

altered olivine-rich rock in Jezero Crater, Mars (NASA). Background images are for illustrative purposes only. Their origins are: stellar nursery Cepheus B (NASA/CXC/PSU/K/JPL-CALTECH/CFA); star HL Tau and its protoplanetary disk (ESO/NAOJ/NRAO/C. BROGAN/B. SAXTON/AUI/NSF); asteroid Vesta (NASA/JPL-CALTECH/UCAL/MPS/DLR/IDA); artist's rendering of Jupiter Trojan asteroids (NASA/JPL-CALTECH); artist's rendering of a cooling planet (NASA/JPL-CALTECH); Mars (ESA/DLR/FU/BERLIN/JUSTIN COWART; CC BY 3.0).

Stony-Iron and Achondrite Meteorites

As accretion progressed, heat from the decay of ²⁶Al and from the transformation of gravitational potential energy allowed some of these planet precursors to undergo differentiation (separation into a dense Fe-Ni core and a silicate mantle), at which point they lost their primitive, chondritic character. Samples of these differentiated planetesimals consist of achondrites, iron meteorites, and stony-irons, which are mixtures of the two.

The stony-iron meteorites preserve information about collisions between planetesimals, a key step in planet formation. These meteorites, subclassified as pallasites or mesosiderites, are mechanical mixtures of silicates and Fe-Ni metal. The pallasites are particularly striking, composed of green, gem-quality olivine grains in a metal matrix (Fig. 1 TOP RIGHT INSET). They were once thought to preserve material from the core-mantle boundary of differentiated asteroids from early in Solar System history. However, current evidence, including oxygen isotope disequilibrium between olivine and metal-derived chromite, is consistent with mixing of an impactor's metallic core with mantle olivine from a parent body (e.g., Windmill et al. 2022). This impact mixing occurred within 10 My of Solar System formation based on ⁵³Mn-⁵³Cr dating of pallasite olivine (Windmill et al. 2022).

Olivine contains enough Mn and Cr in its minor element cache to be an excellent recorder of relative time, as measured by this short-lived, now extinct, 53 Mn- 53 Cr radioisotope system ($t_{1/2}$ = 3.7 My). When combined with absolute age dating from other minerals or bulk rock sources, olivine 53 Mn- 53 Cr dating refines the timing of early Solar System events such as the pallasite-forming impacts noted above. Olivine 53 Mn- 53 Cr dating has also been applied to basaltic achondrite meteorites, including angrites, eucrites, and diogenites, indicating that magmatism was active on planetesimals within 20 My of Solar System formation (e.g., Lugmair and Shukolyukov 1998).

Linking Meteorites to Asteroid Types

Existing asteroids are remnants of both the primitive (chondritic) and differentiated early planetesimals discussed above. As such, they are thought to be the parent bodies of most known meteorites, although linking specific types of meteorites to the asteroid types they come from is a field-wide work in progress. The clearest relationship that has emerged connects the most abundant meteorites, the ordinary chondrites, to S-type asteroids. Variations in the 1- and 2-µm spectral absorption bands of S-type asteroids, measured by VNIR reflectance (Box 1), suggest an olivine to pyroxene ratio consistent with that of ordinary chondrites. Furthermore, returned material from the *Hayabusa* mission to S-type asteroid Itokawa matches the olivine to pyroxene ratio of ordinary chondrites, apparently confirming S-type asteroids as their parent bodies (e.g., Vernazza et al. 2015).

Olivine is also critical to our understanding of differentiated meteorites and asteroids. However, despite the olivine-rich nature of initial, undifferentiated materials (chondrites), the preservation of mantle olivine in pallasites, and the olivine-rich mantle of Earth, spectral studies show that only 0.16% of Main Belt asteroids >2 km in size are olivine-rich (A-types; DeMeo et al. 2019), and dunite-like meteorites of any provenance are rare. This "missing mantle" problem has two interpretations: either olivine-rich mantles are rare, or they are rarely detected (e.g., due to incomplete differentiation of asteroids, whose still-chondritic exteriors are detected by spectroscopic surveys).

Box 1 OLIVINE SPECTROSCOPY

How does the small-scale crystal structure of olivine contribute to our understanding of extraterrestrial materials? The most direct connection is via spectroscopy, or how the atoms and bonds in a crystal interact with light. Olivine is commonly detected and characterized on extraterrestrial bodies through the use of spectroscopy (e.g., reflectance, Raman) in the visible to near infrared (VNIR; 0.5-3 µm) and thermal infrared (TIR; 8-50 µm) wavelength ranges (Fig. 2). In laboratory measurements, the "cross-over," or intermediate infrared wavelengths (4–8 μm) have also been shown to record olivine Fe-Mg composition. This range remains untested in a remote-sensing context but is likely to become a valuable tool for future orbital missions. In the longer (far) IR wavelengths, olivine also has distinctive features (e.g., a 69-µm band) that shift with Fe-Mg composition and have long informed astronomical studies of debris disks and other dusty regions of space (e.g., de Vries et al. 2012). Here, we focus on observations closer to home.

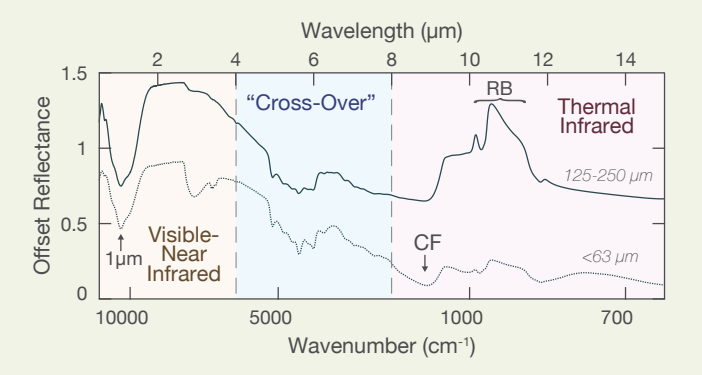


FIGURE 2 Spectra of olivine at VNIR, "cross-over" (intermediate), and TIR wavelengths, for two particle size ranges (<63 μ m and 125–250 μ m). CF = Christiansen feature, RB = reststrahlen band.

The VNIR and TIR spectrometers on telescopes, orbiters, and rovers permit detection and compositional characterization of olivine at a wide range of spatial scales. In VNIR reflectance spectroscopy, olivine has a distinct signature at ~1 µm, which is a composite of three overlapping absorptions that result when incident light causes changes in the valence state of iron. The strength, shape, and position of the ~1-µm band change as a function of olivine abundance, particle size, and Fe-Mg composition. These properties are determined for extraterrestrial objects by comparing remotely sensed spectra to either (1) a suite of laboratory spectra from known materials or (2) spectra calculated using material properties and physical modeling (radiative transfer modeling, e.g., Mustard and Glotch 2019).

Spectroscopy of olivine in the TIR range relies on diagnostic vibrational features (reststrahlen bands) and the emissivity maximum point (Christiansen feature). Reststrahlen bands occur from ~10 to 20 μm in olivine and are useful for determining the Fo content of olivine in the laboratory and, by extension, on planetary objects (Hamilton 2010). These bands are weaker in finer-grained materials, like planetary regolith (FIG. 2), but nonetheless provide information on olivine abundance and Fe-Mg composition (e.g., Koeppen and Hamilton 2008). The Christiansen feature, which occurs at ~8–9 μm in olivine, is generally strong in fine-grained materials, allowing for widespread detection. The wavelength of the Christiansen feature decreases with increasing SiO_2 content of the rock, yielding broad-brush mineralogical insight.

Vesta, one of the largest known asteroids and the parent body of the howardite, eucrite, and diogenite (HED) meteorites, exemplifies the "missing mantle" problem. The HEDs are mostly basaltic, implying that Vesta is differentiated and should have an olivine-bearing mantle. However, direct evidence of such a mantle via remote spectroscopic observations has not been apparent, even though large impacts on Vesta should have been energetic enough to excavate through the crust and expose mantle material. Moreover, the arrival of Dawn to Vesta revealed few olivinerich locations via VNIR spectroscopy, and none within the largest basin (Palomba et al. 2015). In contrast, the more recent discovery of olivine-rich, ultramafic meteorites from Vesta suggests that the asteroid does host an olivinebearing mantle, but likely a small one formed by serial magmatism (Vaci et al. 2021).

Comets

Olivine from comets also plays a key role in understanding early Solar System dynamics, as shown by returned samples of the comet Wild 2 (*Stardust* mission). Along with the expected interstellar or presolar grains, these samples contain rocky material that is similar in mineralogy to chondrules and must have originated in hotter regions closer to the Sun. Olivine Mn/Fe ratios vary greatly between grains, suggesting a plethora of crystal origins, including three chondrite types and at least one unknown source (Brownlee and Joswiak 2017). Wild 2 likely comprises materials spanning the entire solar nebula, demonstrating that system-scale mixing and migration were important early Solar System processes.

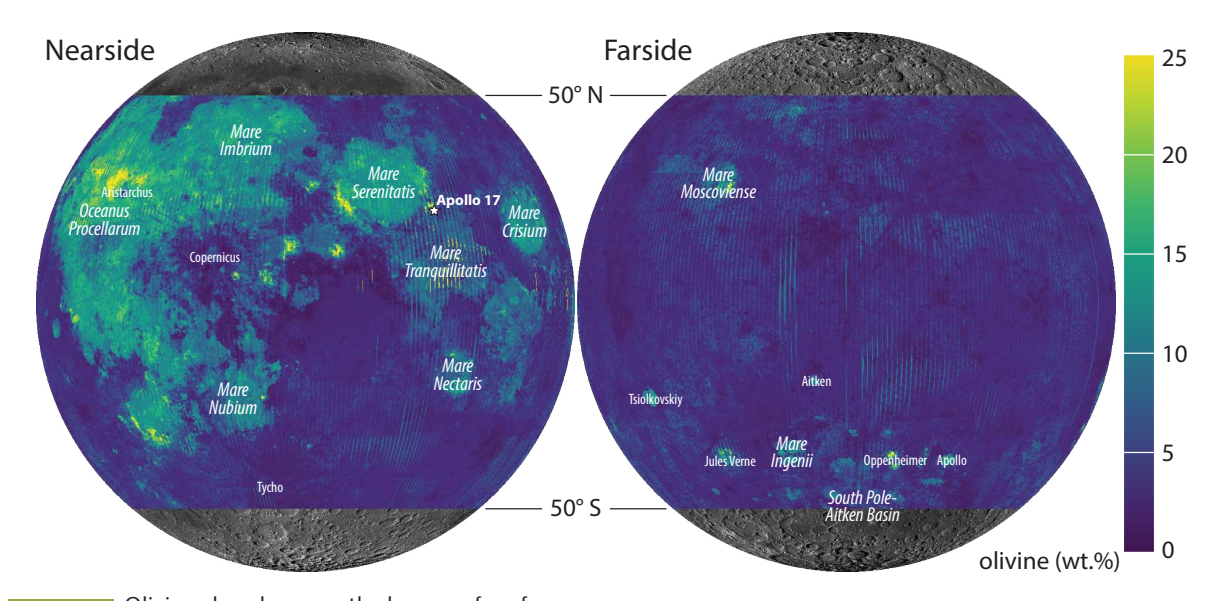
THE MOON

Earth's Moon offers us an opportunity to study a larger, differentiated body that exposes both primary and secondary crusts, and is close enough to invite iterative robotic and crewed missions. The Moon formed ~100 My after the Sun from a collision between a Mars-sized body, Theia, and the proto-Earth. In the resultant lunar magma ocean (LMO), iron settled out to form a small core, followed by a crystallization sequence that produced the

lunar mantle and primary crust. Experiments and models based on estimates of the lunar bulk composition show that Mg-rich olivine was the first mineral to crystallize and sink from the LMO, followed by pyroxene and more Fe-rich olivine (e.g., Charlier et al. 2018). At ~80% LMO crystallization, plagioclase formed, floated to the surface, and accumulated as the Moon's primary anorthosite crust. Finally, ilmenite crystallized and contributed to gravitational instability and a large-scale overturn of the mantle.

Olivine and pyroxene Mg# (molar Mg/(Mg + Fe²⁺)) are critical for identifying primary crustal rocks, known as ferroan anorthosites. The presence of Fe-rich olivine and pyroxene (Mg# 50–70) alongside dominant anorthite supports the idea that such rocks represent the original flotation crust that formed during late-stage LMO crystallization. However, Mg-rich olivine and pyroxene (up to Mg# ~90) occur in some anorthosites discovered in lunar meteorites (e.g., Gross et al. 2014). The presence of these "magnesian anorthosite" clasts adds complexity to LMO crystallization models, requiring more compositional heterogeneity during cooling and crustal accumulation.

Samples of the lunar mantle would provide direct evidence of its mineralogy and chemistry. But despite a high presumed abundance, definitive identification of mantle olivine has proven elusive. Most cumulate olivine in the lunar sample suite is consistent with a secondary crustal origin. Additionally, global spectral datasets fail to identify ultramafic (i.e., olivine-rich) material on the innermost rings of large impact basins, which would have excavated the upper mantle (Lemelin et al. 2019; FIG. 3). Furthermore, the mafic component of the lunar highlands and the largest basin, South Pole-Aitken, is dominated by low-calcium pyroxene rather than olivine, suggesting a spatially heterogeneous or even pyroxene-dominated upper mantle (e.g., Lemelin et al. 2019). Inefficient mantle overturn could explain this unexpected mineralogy, but it also harkens back to the "missing mantle" problem of Vesta and the asteroid belt in general.



Olivine abundance on the lunar surface from 50° N to 50° S, derived from JAXA SELENE/ Kaguya Multiband Imager reflectance data (Lemelin et al. 2019). Olivine is concentrated in the lunar maria. Created with Lunar QuickMap using orthographic projections and LROC base map, data overlay at 100% opacity.

Although direct study of mantle olivine is difficult, the products of its partial melting and subsequent evolution are more accessible. For example, detailed electron microscopy and X-ray element mapping of lunar troctolite 76535 (Fig. 1, Rightmost inset) reveal olivine with complex zoning of phosphorus. Variations in the incorporation of this trace element broadly record conditions and rates of olivine growth, in this case suggesting an unexpectedly rapid and complicated cooling history, with periods of olivine dissolution and reprecipitation (Nelson et al. 2021). These findings suggest that some intrusive lunar rocks crystallized and obtained their unique geochemical signatures in small, reactive melt lenses within crustal and upper mantle cumulates.

Back on the Moon's surface, olivine is more abundant in the basalt-dominated mare regions (secondary crust) relative to the anorthositic lunar highlands (primary crust) (Lemelin et al. 2019; Fig. 3). In mare rocks, olivine composition tracks mantle source regions and subvolcanic plumbing, as it does on Earth. Olivine in the pyroclastic "orange glass" deposit from Apollo 17 (Fig. 1, Center Inset) preserves primitive melt inclusions containing >1000 ppm H₂O, showing that parts of the lunar interior could contain as much water as Earth's mid-ocean ridge basalt (MORB) mantle (Hauri et al. 2017). The "wet" Moon implied by these findings is inconsistent with wholesale volatile loss due to giant impact and supports either a less energetic formation scenario or a later, meteorite-derived volatile addition to the Moon (a "late veneer").

MARS

Like the Moon, Mars had a magma ocean early in its history and later volcanism was primarily basaltic. From there, Mars evolved beyond a secondary crust to the formation of sedimentary rocks and highly weathered surfaces. Weathering of iron-bearing olivine even contributes to the rusty dust that gives Mars its "red planet" moniker.

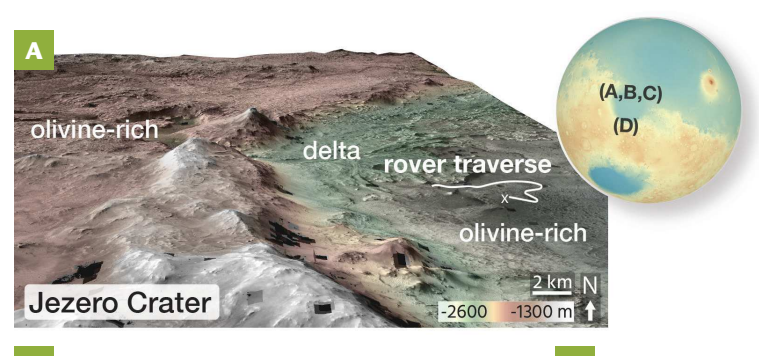
Olivine has been detected on Mars through orbital and in-situ (rover and lander) studies, as well as in Martian meteorites. Olivine is widespread on the Martian surface, with several notable remotely detected concentrations, based on TIR and VNIR data: (1) in deposits circumferential to the large impact basins Isidis, Hellas, and Argyre; (2) in inter-crater plains in the ancient (~3–4 Gy), heavily cratered southern highlands; (3) in deposits along the floor of the 4000-km-long Valles Marineris; and (4) in crater ejecta and unconsolidated sand deposits in the northern highlands (e.g., Koeppen and Hamilton 2008). Olivine has also been detected by rovers in several locations on Mars, including at Gusev Crater by *Spirit*, Gale Crater by *Curiosity*, and Jezero Crater by *Perseverance* (e.g., McSween 2015).

Olivine detection is not limited to a binary result. For example, Koeppen and Hamilton (2008) used TIR spectral endmembers (e.g., Fo₉₁, Fo₆₈, Fo₃₉) to constrain the composition of olivine detected by Mars Global Surveyor to within ~10–20 mol% Fo, revealing that the most Mg-rich olivine deposits occur circumferential to Mars' large impact basins, intermediate compositions are the most widespread across the planet's surface, and olivine more Fe-rich than ~Fo₂₅ is rare. The relatively high-Mg olivine deposits have been traditionally interpreted as exhumed upper mantle (e.g., Ehlmann and Edwards 2014), apparently corroborating the models of Mars' primordial magma ocean where Mg-rich cumulates settled out first and, during subsequent overturn, ascended to form the upper mantle. The intermediate Fe-Mg compositions of olivine detected remotely across Mars, conventionally interpreted as the products of extrusive volcanism, complicate this story of magma ocean

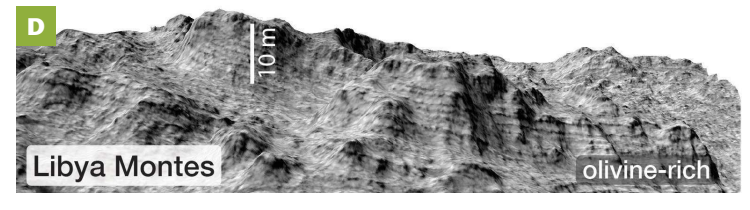
overturn by implying that Fe-rich cumulates remained at sufficiently shallow depths in the mantle to participate in surface magmatism. Likewise, the intermediate compositions of olivine found at Gusev Crater (~Fo $_{40-70}$) and measured in Martian meteorites, such as lherzolitic/poikilitic shergottites (~Fo $_{65-80}$) (McSween 2015), imply a poorly mixed, compositionally heterogeneous Martian mantle.

Martian meteorites are a varied group, but chiefly composed of the SNCs: basalts and gabbros (shergottites), clinopyroxenites (nakhlites), and dunites (chassignites) (e.g., McSween 2015). The Chassigny dunite is not a mantle rock but an olivine cumulate from a basaltic magma, and estimates of its parental composition are alkaline, similar to Gusev rocks. However, the whole rock composition of one olivine-phyric shergottite, Yamato 980459, is interpreted as a primary magma composition, implying that phase equilibrium experiments on this composition can predict mantle mineralogy. Such experiments reveal that olivine and orthopyroxene co-exist in Mars' upper mantle at depths of 85–100 km (e.g., McSween 2015).

Uncertainties remain about the composition and geologic context of olivine on and within Mars. Most remote estimates of olivine composition on Mars using VNIR and TIR spectroscopy are complicated by confounding variables including mineral abundance and particle size, which add uncertainty to the quantification of Fe-Mg content. The origin of olivine-rich rocks on Mars is also an active area of study. Orbital investigations of Mars have suggested







Olivine-bearing rocks in and near the Nili Fossae region of Mars. (A) Digital terrain model (DTM) of Jezero Crater and Nili Planum, with landing site ("x") and traverse of the *Perseverance* rover in white. Much of the region is covered in a thin (~1–10 m) layer of olivinerich rock. (B) Outcrops of olivine-rich basaltic rocks at Jezero Crater (DTM from rover images). (C) Olivine grains from rock in (A) and (B). (D) Layered olivine-rich rock, stratigraphically correlated with rocks in/near Jezero Crater (DTM from orbital data).

that many supposed lava flows on Mars may be clastic rocks, including the thinly layered, highly friable, olivine-rich deposits circumferential to the Isidis Basin (Kremer et al. 2019) (FIG. 4). Meanwhile, recent in situ observations by the *Perseverance* rover at Jezero Crater reveal that at least some local deposits of these supposed sedimentary rocks may be layered cumulates (Liu et al. 2022). Return of samples cached by *Perseverance* will permit microanalysis, enhancing our models for the origin of olivine-rich rocks on Mars.

Mysteries also remain regarding the nature of aqueous activity on Mars as revealed by the distribution and alteration of olivine. Although Mars' water-eroded landforms and hydrous minerals indicate prolonged subsurface and surficial water activity, widespread detection of olivine indicates that the total extent of weathering on the planet must have been limited (Hoefen et al. 2003). Alteration products of olivine (e.g., serpentine, smectite clays, oxides, sulfates) have been identified on the surface of Mars, but the geological settings and conditions of alteration remain ambiguous.

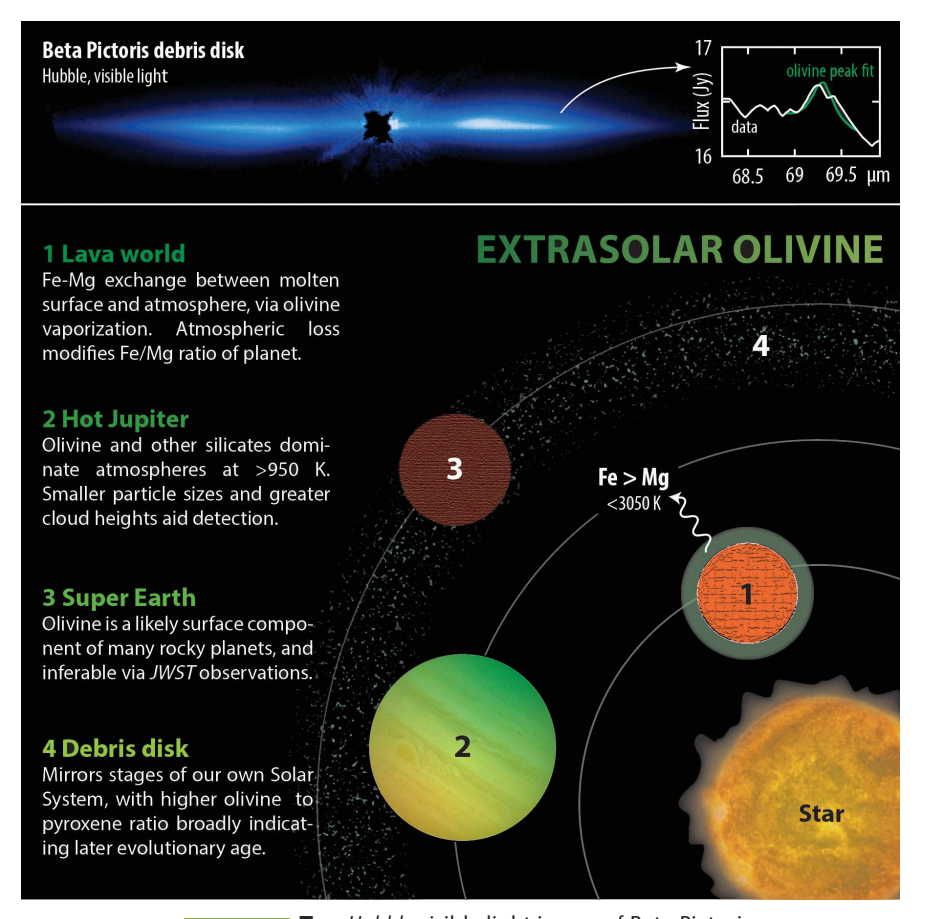
VENUS

As on Mars, the weathering rates of olivine constrain timescales of surface processes on Venus. Venus has a dense, CO₂-rich atmosphere that precludes surface observa-

tion at most optical remote sensing wavelengths. However, ESA's *Venus Express* observed the Venusian surface over a spectral window at ~1 μm , revealing high emissivity values suggestive of surface olivine and pyroxene. Under a Venuslike atmosphere, it takes only a few years for olivine to weather into hematite or magnetite, which have much lower emissivity at ~1 μm (Filiberto et al. 2020). Thus, if confirmed, the presence of olivine on the surface of Venus would imply that some regions have surfaces less than a few years old. In other words, definitive detection of olivine will demonstrate that Venus is geologically active.

OLIVINE BEYOND OUR SOLAR SYSTEM

As technological advances enable science to extend farther from our home planet, researchers have begun to detect and model olivine in other stellar systems (Fig. 5). Olivine is expected to be present on and in many rocky exoplanets, as it is in our own Solar System. It might even occur above the rocky and molten surfaces of planets. The atmospheres of K2-141b and several other "lava ocean planets" (planets with molten daysides; Léger et al. 2011) are thought to contain silicate vapor, which may condense to form clouds of crystals at night. Experiments on olivine vaporization kinetics imply that atmospheric loss from lava worlds can modulate planet-wide Fe/Mg ratios. At temperatures below 3050 K, lava worlds should be enriched in Mg relative to their initial bulk composition due to preferential loss of Fe from vaporizing olivine (Fig. 5; Costa et al. 2017). Atmospheric microphysics modeling shows that hot, giant exoplanets (similar to Jupiter in size, but with shorter orbital periods than Mercury) are likely to have atmospheres dominated by olivine and other silicates in the layers hotter than 950 K (Gao et al. 2020). Finally, olivine signatures appear in infrared spectra of "dusty" stellar systems, that is, stars with surrounding debris disks (e.g., de Vries et al. 2012). The total olivine to pyroxene ratio of these systems and other



TOP: Hubble visible light image of Beta Pictoris debris disk (NASA/ESA/UNIVERSITY OF ARIZONA) with corresponding far IR olivine spectrum (DE VRIES ET AL. 2012). **Воттом**: Overview of olivine in exoplanetary settings.

planetary objects is broadly correlated with evolutionary age, allowing identification of extrasolar analogs for many stages of Solar System evolution, from the protoplanetary era, to terrestrial planet formation, migration of giant planets, and stellar death (e.g., Lisse et al. 2012).

FUTURE DIRECTIONS

As the promise of farther reaching and more detailed exploration of olivine in planetary materials comes to fruition, scientists and mission planners must strike a balance between acquisition of broad, high-coverage data at global or system scales and spatially limited, in-depth data at outcrop to atomic scales. With this balance in mind, the future of olivine in planetary science rests on four key pillars: (1) continuing analysis of existing samples and data, which are far from exhausted in their potential; (2) building more complete laboratory databases of olivine and olivine-bearing materials, both spectroscopic and petrologic, for extraterrestrial compositions, temperatures, fO_2 , etc.; (3) technological advances to improve remote sensing capabilities; and (4) explicit incorporation of tools to study olivine in future ground- and space-based missions.

Ongoing and upcoming missions highlight the interaction of these four pillars. With unprecedented reach and resolution, the *James Webb Space Telescope (JWST)* has given us VNIR and TIR spectra of stars and exoplanet atmospheres, including some "silicate" detections. Disk-averaged spectra of rocky planets are expected in 2023. Given well-chosen targets, olivine detection in any of these galactic

materials is possible with the JWST. Closer to the Sun, in 2025, the BepiColombo mission will begin acquiring spectra (including TIR) of Mercury's surface, which existing petrologic models suggest could contain olivine. BepiColombo data will allow us to assess and refine those models and to consider additional conditions to study in the laboratory. Current uncrewed missions to the Moon (e.g., Chang'e sample returns) have added diversity to the cache of lunar samples available for in situ laboratory analysis and bolstered our understanding of regions of the Moon not visited by Apollo. Continuing analysis of these newer samples along with updated analytical work on Apollo rocks paves the way for Artemis, which will send human explorers back to the Moon for the first time in 50 years. Perhaps they will discover the first in situ mantle xenoliths, magnesian anorthosites, or a host of primitive, olivine-bearing pyroclastic deposits.

It is critical that olivine research continues and expands into specific planetary realms. Although Earth-centric ideas and planetary analogs have proven valuable, they are self-limiting at best and misleading at worst. As we have seen many times with Earth-based spectral libraries, petrologic studies, and even basic assumptions about planetary differentiation, what we think we know about olivine and its formation environments can be blown away by the swirling winds and magma seas of distant worlds and distant time.

ACKNOWLEDGMENTS

ECF is grateful to the Heising-Simons Foundation and to Esteban Gazel for support via a 51 Pegasi b Fellowship (Cornell University). We acknowledge the use of imagery from Lunar QuickMap (https://quickmap.lroc.asu.edu), a collaboration between NASA, Arizona State University, and Applied Coherent Technology Corp. We thank Guy Libourel and an anonymous reviewer for constructive feedback that improved this contribution.

REFERENCES

- Brownlee DE, Joswiak DJ (2017) Diversity of the initial rocky planetary building materials at the edge of the solar system. Meteoritics and Planetary Science 52: 471-478, doi: 10.1111/maps.12804
- Charlier B, Grove TL, Namur O, Holtz F (2018) Crystallization of the lunar magma ocean and the primordial mantle-crust differentiation of the Moon. Geochimica et Cosmochimica Acta 234: 50-69, doi: 10.1016/j.gca.2018.05.006
- Costa GCC, Jacobson NS, Fegley Jr. B (2017) Vaporization and thermodynamics of forsterite-rich olivine and some implications for silicate atmospheres of hot rocky exoplanets. Icarus 289: 42-55, doi: 10.1016/j.icarus.2017.02.006
- DeMeo FE and 7 coauthors (2019) Olivine-dominated A-type asteroids in the main belt: distribution, abundance and relation to families. Icarus 322: 13-30, doi: 10.1016/j.icarus.2018.12.016
- de Vries BL and 22 coauthors (2012) Cometlike mineralogy of olivine crystals in an extrasolar proto-Kuiper belt. Nature 490: 74-76, doi: 10.1038/nature11469
- Ehlmann BL, Edwards CS (2014) Mineralogy of the Martian surface. Annual Review of Earth and Planetary Sciences 42: 291-315, doi: 10.1146/ annurev-earth-060313-055024
- Faure F, Auxerre M, Casola V (2022) Slow cooling during crystallisation of barred olivine chondrules. Earth and Planetary Science Letters 593: 117649, doi: 10.1016/j. epsl.2022.117649
- Filiberto J, Trang D, Treiman AH, Gilmore MS (2020) Present-day volcanism on Venus as evidenced from weathering rates of olivine. Science Advances 6: eaax7445, doi: 10.1126/sciadv.aax7445
- Gao P and 8 coauthors (2020) Aerosol composition of hot giant exoplanets dominated by silicates and hydrocarbon hazes. Nature Astronomy 4: 951-956, doi: 10.1038/s41550-020-1114-3
- Gross J, Treiman AH, Mercer CN (2014) Lunar feldspathic meteorites: constraints on the geology of the lunar highlands, and

- the origin of the lunar crust. Earth and Planetary Science Letters 388: 318-328, doi: 10.1016/j.epsl.2013.12.006
- Hamilton VE (2010) Thermal infrared (vibrational) spectroscopy of Mg–Fe olivines: a review and applications to determining the composition of planetary surfaces. Geochemistry 70: 7-33, doi: 10.1016/j. chemer.2009.12.005
- Hauri EH and 6 coauthors (2017) Origin and evolution of water in the Moon's interior. Annual Review of Earth and Planetary Sciences 45: 89-111, doi: 10.1146/ annurev-earth-063016-020239
- Hoefen TM and 5 coauthors (2003) Discovery of olivine in the Nili Fossae region of Mars. Science 302: 627-630, doi: 10.1126/science.1089647
- Koeppen WC, Hamilton VE (2008) Global distribution, composition, and abundance of olivine on the surface of Mars from thermal infrared data. Journal of Geophysical Research: Planets 113: E5, doi: 10.1029/2007IE002984
- Kremer CH, Mustard JF, Bramble MS (2019) A widespread olivine-rich ash deposit on Mars. Geology 47: 677-681, doi: 10.1130/ G45563.1
- Léger A and 25 coauthors (2011) The extreme physical properties of the CoRoT-7b super-Earth. Icarus 213: 1-11, doi: 10.1016/j. icarus.2011.02.004
- Lemelin M and 5 coauthors (2019) The compositions of the lunar crust and upper mantle: spectral analysis of the inner rings of lunar impact basins. Planetary and Space Science 165: 230-243, doi: 10.1016/j. pss. 2018.10.003
- Libourel G, Portail M (2018) Chondrules as direct thermochemical sensors of solar protoplanetary disk gas. Science Advances 4: eaar3321, doi: 10.1126/sciadv.aar3321
- Lisse CM and 9 coauthors (2012) *Spitzer* evidence for a late-heavy bombardment and the formation of ureilites in η Corvi at ~1 Gyr. The Astrophysical Journal 747: 93, doi: 10.1088/004-637X/747/2/93
- Liu and 70 coauthors (2022) An olivine cumulate outcrop on the floor of Jezero crater, Mars. Science 377: 1513-1519, doi: 10.1126/science.abo2756

- Lugmair GW, Shukolyukov A (1998) Early solar system timescales according to 53 Mn- 53 Cr systematics. Geochimica et Cosmochimica Acta 62: 2863-2886, doi: 10.1016/S0016-7037(98)00189-6
- McSween Jr. HY (2015) Petrology on Mars. American Mineralogist 100: 2380-2395, doi: 10.2138/am-2015-5257
- Messenger S, Keller LP, Lauretta DS (2005) Supernova olivine from cometary dust. Science 309: 737-741, doi: 10.1126/ science.1109602
- Mustard JF, Glotch TD (2019) Theory of reflectance and emittance spectroscopy of geologic materials in the visible and infrared regions. In: Bishop JL, Bell III JF, Moersch JE (eds) Remote Compositional Analysis. Cambridge University Press, Cambridge, pp 21-41, doi: 10.1017/9781316888872.004
- Nelson WS, Hammer JE, Shea T, Hellebrand E, Taylor GJ (2021) Chemical heterogeneities reveal early rapid cooling of Apollo Troctolite 76535. Nature Communications 12: 7054, doi: 10.1038/s41467-021-26841-4
- Nittler LR, Ciesla F (2016) Astrophysics with extraterrestrial materials. Annual Review of Astronomy and Astrophysics 54: 53-93, doi: 10.1146/annurev-astro-082214-122505
- Palomba E and 11 coauthors (2015)
 Detection of new olivine-rich locations on Vesta. Icarus 258: 120-134, doi: 10.1016/j. icarus. 2015.06.011
- Vaci Z and 9 coauthors (2021) Olivine-rich achondrites from Vesta and the missing mantle problem. Nature Communications 12: 5443. doi: 10.1038/s41467-021-25808-9
- Vernazza P, Zanda B, Nakamura T, Scott E, Russell S (2015) The formation and evolution of ordinary chondrite parent bodies. In: Michel P, DeMeo FE, Bottke WF (eds) Asteroids IV. University of Arizona Press, Tucson, pp 617-634
- Windmill RJ and 7 coauthors (2022) Isotopic evidence for pallasite formation by impact mixing of olivine and metal during the first 10 million years of the Solar System. PNAS Nexus 1: pgac015, doi: 10.1093/pnasnexus/pgac015 ■